PHYSICAL REVIEW B **74**, 121411(R) (2006)

Temperature dependence of the optical excitation lifetime and band gap in chirality assigned semiconducting single-wall carbon nanotubes

Ferenc Simon,* Rudolf Pfeiffer, and Hans Kuzmany
Institut für Materialphysik, Universität Wien, Strudlhofgasse 4, A-1090 Wien, Austria
(Received 25 May 2006; revised manuscript received 21 July 2006; published 27 September 2006)

The temperature dependence of optical excitation lifetime $1/\Gamma$ and transition energies E_{ii} were measured for bucky papers of single-wall carbon nanotubes (SWCNTs) and inner tubes in double-wall carbon nanotubes (DWCNTs) using resonant Raman scattering on the radial breathing mode. The temperature dependence of Γ and E_{ii} is the same for both types of samples and is independent of tube chirality. The data suggest that electron-phonon interaction is responsible for the temperature dependence of E_{ii} and Γ. The temperature independent contribution to Γ is much larger in SWCNT than in DWCNT samples. This is explained by the different nanotube environment in the two types of samples. Γ for the inner tubes of the DWCNTs is only ~30 meV below 150 K, which is comparable to that found for individual SWCNTs and is considered as intrinsic to the tubes.

DOI: 10.1103/PhysRevB.74.121411 PACS number(s): 73.63.Fg, 78.67.−n, 78.30.−j

Single-wall carbon nanotubes (SWCNTs) have been in the focus of interest in the last decade due to their unique physical and chemical properties, which makes them a potential candidate for a broad range of applications.[1] It is now established theoretically[2] and there is emerging experimental evidence[3] that excitonic effects, i.e., the correlation of photoexcited electrons and holes, play an important role in the optical absorption and emission properties of SWCNTs. The lifetime of the excitons τ_{exciton}, the optical excitation energies E_{ii}, and their temperature dependencies are crucial parameters for the optoelectronic applications of SWCNTs. SWCNTs are characterized by a great variation of physical properties depending on the (n,m) chiral indices. Therefore chirality assigned determination of these parameters is vital. τ_{exciton} was measured in time-resolved photoexcited studies[4–6] and estimated theoretically.[7,8] E_{ii} was measured using photoluminescence spectroscopy in a chirality assigned manner for ensembles of isolated SWCNTs (Ref. 9) and for individual SWCNTs.[10,11]

The scattering rate of the optically excited states $\Gamma=1/\tau$ is related to τ_{exciton}, although the relationship has not been fully described theoretically. Both Γ and E_{ii} are accessible from resonant Raman scattering (RRS) studies.[12,13] Such studies have been presented on surfactant separated[14,15] and also for bucky-paper SWCNT samples.[14] The temperature dependence, studied using varying laser powers, of E_{ii} was found to markedly differ for $\nu=1$ and $\nu=2$ type semiconducting SWCNTs, where ν is given by $(n-m)\text{mod}\,3=\nu$. $\nu=1$ tubes were found to blueshift, whereas $\nu=2$ to redshift with increasing temperature. In contrast, in a recent study E_{ii} was found to redshift for both $\nu=1,2$ with increasing temperature for individual SWCNTs,[16] which was explained by the electron-phonon coupling.[16,17] Clearly, the role for the tube environment requires further studies. In addition, no temperature dependent measurement of Γ on chirality assigned SWCNTs is available.

Here, the temperature (T) dependence of the (n,m) specific electronic transitions and scattering rates for optical excitations is reported for SWCNTs in different environments. We measured SWCNTs with the same chirality in bucky-paper SWCNT samples and as inner tubes in double-wall carbon nanotube (DWCNT) samples. The latter type of sample has attracted considerable interest as the inner tubes are in a well-shielded environment, which results in exceptionally long phonon lifetimes.[18] Also, whereas a carbon nanotube in a SWCNT sample is surrounded by other tubes with random chiralities, a given inner tube is embedded in an outer tube with a well defined chirality. The outer tubes provide a well defined and measurable radial pressure to the inner tube.[19] As a consequence, the narrow Raman lines of the inner tubes allow to study distinct inner-tube Raman spectra of tube pairs.[18,19] We observe a large inhomogeneous contribution to Γ for the SWCNT sample but the same T dependence as for the inner tubes in the DWCNTs. The same T dependence of E_{ii} was observed for both types of samples. These results suggest that both E_{ii} and the T dependent part of Γ are independent of the tube environment. A common and robust mechanism such as electron-phonon interaction is therefore likely to be responsible for them.

The studied SWCNTs were HiPco (CNI, Houston, USA) and CoMoCat samples (SWeNT, Oklahoma, USA) with mean tube diameters of $d=1.0$ and 0.8 nm, respectively, as determined from a Raman analysis.[13] DWCNTs were produced by heating SWCNTs (Nanocarblab, Moscow, Russia, $d=1.4$ nm) encapsulating fullerenes ("peapods"[20]) at 1270 °C for 2 h. The peapods are prepared by heating SWCNT with C_{60} at 650 °C for 2 h in a sealed ampoule.[21] The mean diameter of the inner tubes is $d=0.7$ nm,[22] thus d is very similar for the inner tubes and the two SWCNTs samples. The Raman spectrometer was a Dilor *xy* triple grating instrument excited by a tunable laser in the 2.01–2.18 eV (616–568 nm) range with 22 laser energies. The spectrometer was operated in the "macro" mode with low laser power densities of 5 mW/(100 μm)^2 to avoid sample heating. Discharge calibration lamps and Si powder were used to calibrate the Raman shifts and intensities, respectively. Measurements were performed in the 80–600 K temperature range in a home-built cryostat.

In Fig. 1 we show the energy dispersive Raman map for the SWCNT (CoMoCat) and DWCNT samples for a part of

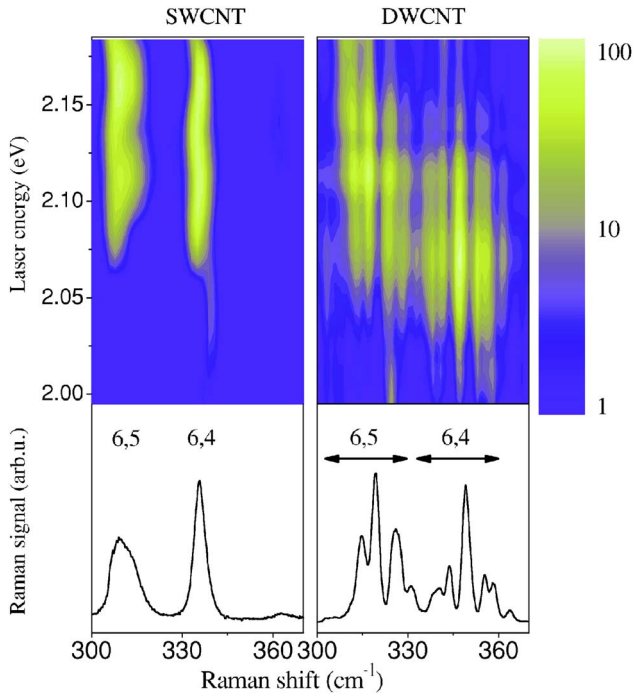

FIG. 1. (Color online) Energy dispersive Raman contour plot for SWCNT (CoMoCat) and DWCNT samples at 80 K. The vertical bar shows the color coding for the observed intensities on a logarithmic scale in arbitrary units. Lower panels show individual Raman spectra with 2.10 eV laser energy.

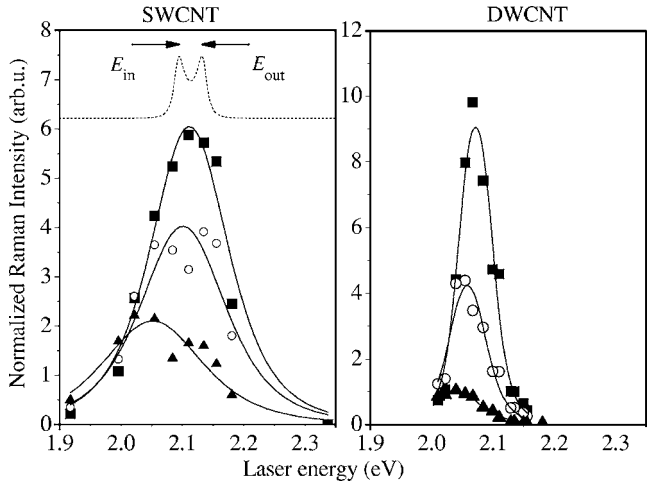

FIG. 2. Raman resonance profile for the (6,4) tubes in the SWCNT (CoMoCat) and DWCNT samples ■: 80 K, ○: 300 K, ▲: 600 K. Solid curves show fits with the RRS theory. Dashed curve is a simulation for the 80 K SWCNT data with $\Gamma=10$ meV. Arrows indicate the incoming and outgoing resonance energies. Note the much narrower widths for the DWCNT sample.

the radial breathing mode (RBM) and excitation energy range at 80 K. Similar contour plots showing a larger area, have been used to assign (n,m) indexes to the different nanotubes in SWCNT (Refs. 14 and 15) and DWCNT samples.[19] The two peaks at 310 and 337 cm^{-1} with 2.12 and 2.08 eV transition energies correspond to the E_{22} optical transition enhanced RBMs of the (6,5) and (6,4) tubes for the SWCNT sample.[14,15] These two tubes are representative for both semiconducting SWCNT classes $\nu=1$ and $\nu=2$ and their RBMs are well separated from all other tube modes. This renders them ideal for studying the T dependent RRS. For the DWCNT, (6,5) and (6,4) are inner tubes and their RBMs are split into several components as the same inner tube can be in several outer ones.[19,23] The difference in the resonance energies results from the different environment for the two samples: an outer tube for the DWCNT sample and the surrounding ensemble of the other SWCNTs for the SWCNT sample. The gradual redshift for the inner tube resonance energies with increasing Raman shift was associated to the pressure induced by the outer tubes.[19]

The temperature dependence of the Raman contour plots was measured for all three samples. Raman intensities corresponding to individual modes were determined by fitting Voigtian line shapes whose Gaussian component was given by the residual spectrometer resolution. The energy dependent Raman intensities for two particular tube modes in the two kinds of samples are shown in Fig. 2 as a function of T. For the SWCNT CoMoCat sample, the (6,4) tube mode at 337 cm^{-1} is shown and the strongest (6,4) inner tube component at 347 cm^{-1} is shown for the DWCNT sample. The T dependent resonant Raman data can be fitted with the resonance Raman theory for Stokes Raman modes[12,13]

$$I(E_l) = M_{eff}^4 \left| \frac{(E_l - E_{ph})^4 [n_{\mathrm{BE}}(E_{ph}) + 1]}{(E_l - E_{ii} - i\Gamma)(E_l - E_{ph} - E_{ii} - i\Gamma)} \right|^2. \quad (1)$$

Here, the electronic density of states of SWCNTs is assumed to be a Dirac function and the effective matrix element M_{eff}, describing the electron-phonon interactions is taken to be independent of T and energy. E_l, E_{22}, and E_{ph} are the exciting laser, the optical transition and the phonon energies, respectively. $n_{\mathrm{BE}}(E_{ph})=[\exp(E_{ph}/k_BT)-1]^{-1}$ is the Bose-Einstein function and accounts for the thermal population of the vibrational state[24] and $n_{\mathrm{BE}}(E_{ph})+1$ changes a factor ~ 2 between 80 and 600 K. The T dependence of E_{ph} is $\sim 1\%$ for the studied T range[25] thus it can be neglected. The first and second terms in the denominator of Eq. (1) describe the incoming and outgoing resonances, respectively and are indicated on a simulated curve by arrows in Fig. 2. These are separated by E_{ph}. This means the apparent width of the resonance Raman data does not represent Γ.

Solid curves in Fig. 2 show fits for the given RBMs at all temperatures simultaneously, i.e., with the same matrix element, using Eq. (1) and thus allow us to derive the T dependence for E_{22} and Γ. The result for the T dependent relative optical transition energies $E_{22}(T)-E_{22}(80\ \mathrm{K})$ and $\Gamma(T)$ is summarized in Fig. 3. The room temperature values of E_{22} are given in Table I together with the Γ_0 and Γ_1 parameters which describe the T dependence of Γ and are discussed below in detail.

We start the discussion with the T dependent optical transition energies. Differences between the room temperature values for E_{22}'s for DWCNT,[19] SWCNT in bucky paper, and as dispersed[14] have been previously observed and explained by the effect of the different environment. The surprising observation is the overall redshift of 50(10) meV between 80

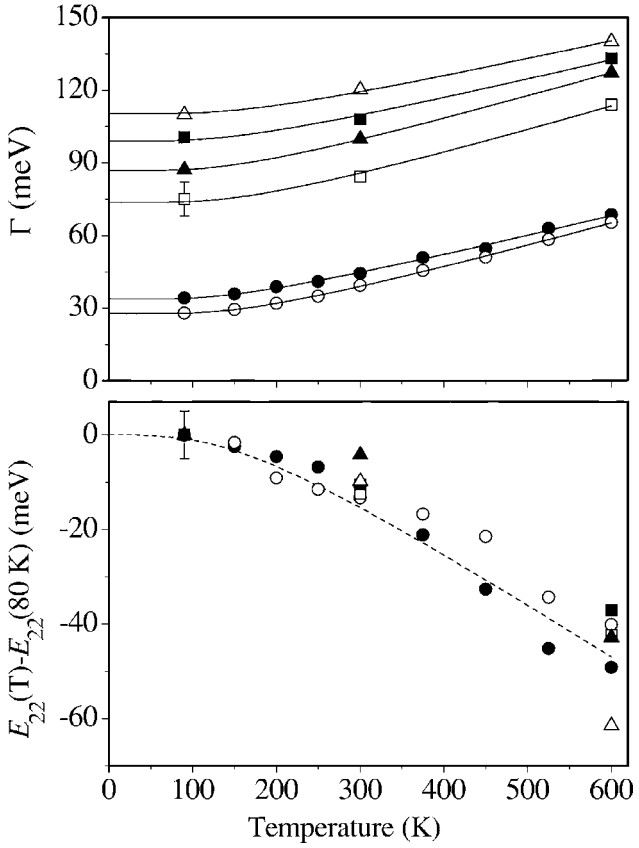

FIG. 3. Temperature dependence of the optical transition energy shift $E_{22}(T)-E_{22}(80\ \mathrm{K})$ and the damping parameter Γ for the (6,5) and (6,4) inner tubes of DWCNTs, HiPco tubes, and CoMoCat tubes. Open and closed symbols are for the (6,4) and (6,5) tubes, respectively. △: CoMoCat, □: HiPco, ○: DWCNT. Solid curves are calculated values of $\Gamma(T)$ as explained in the text. Dashed curve is the calculated redshifting E_{22} for a (6,5) tube as explained in the text. Representative error bars for both parameters are shown. The error bars are similar to the symbol size for $\Gamma(T)$ of inner tubes.

and 600 K irrespective of the sample type and the family of tube, $\nu=1$ or 2. Recently, ~50 meV redshifts were observed for individual suspended nanotubes using the same method for SWCNTs with $\nu_{\mathrm{RBM}}>250\ \mathrm{cm}^{-1}$.[16] The observed T dependence was explained by the softening of the band gap at high temperatures due to electron-phonon coupling[16,17] yielding the optical transition energy shift

$$\Delta E_{22}(T)=\alpha_1\Theta_1 n_{\mathrm{BE}}(k_B\Theta_1)+\alpha_2\Theta_2 n_{\mathrm{BE}}(k_B\Theta_2). \quad (2)$$

In Fig. 3, we show the calculated $\Delta E_{22}(T)$ for a (6,5) tube using Eq. (2) with parameters given in Ref. 17: $\alpha_1=-1.17\times10^{-5}$ eV/K, $\alpha_2=-1.04\times10^{-4}$ eV/K, $\Theta_1=103.8$ K, and $\Theta_2=487.4$ K. Since $\Delta E_{22}(80\ \mathrm{K})\approx\Delta E_{22}(0\ \mathrm{K})$ plotting $\Delta E_{22}(T)$ on the $E_{22}(T)-E_{22}(80\ \mathrm{K})$ data is justified. A similar calculation for a (6,4) tube does not give a significantly different curve. A good agreement between the experimental points and the calculation is observed, which confirms the validity of the theoretical explanation presented in Ref. 17. Both ours and the results in Ref. 16 are in difference to a previous study in which a blueshift with increasing T was reported for $\nu=1$ tubes in a laser heated sample.[14]

Our result confirms the redshift of optical transition energies with increasing T as observed on individual tubes.[16] It holds for SWCNTs in bucky papers and for inner tubes surrounded by outer tubes in DWCNT samples. It thus unambiguously proves that electron-phonon interaction is the dominant mechanism for the T variation of the optical transitions. Other effects such as thermal expansion do not play a role even though radial pressure is present.

$\Gamma(T)$ can be separated into a residual Γ_0 and a T dependent part and it can be fitted empirically with

$$\Gamma(T)=\Gamma_0+\Gamma_1 n_{\mathrm{BE}}(E_{ph}). \quad (3)$$

Equation (3) assumes that the T dependence of Γ is caused by electron-phonon coupling whose strength is given by a broadening parameter Γ_1 and the phonon population. The T dependence of the latter is described by the Bose-Einstein function. Naturally, a comprehensive theory beyond our empirical fit is required to better describe this phenomenon. Nevertheless, fits using Eq. (3) describe the measured data reasonably well as shown in Fig. 3 with solid curves. The values for Γ_0 and Γ_1 are given in Table I. The residual Γ_0 shows marked differences for the three samples. In contrast, the T dependence, given by Γ_1 is similar for all samples and chiralities studied and scatters in the 40–50 meV range. We assign the T dependent part of $\Gamma(T)$ to homogeneous broadening thus to a true lifetime effect.

The low value of Γ_0 for individual SDS dispersed SWCNTs and inner tubes in DWCNTs and its high value for the two bucky-paper samples of SWCNTs can be explained by the sample morphologies assuming that nearest neighbor tube-tube interactions strongly affect the transition energies.

TABLE I. Phonon energies E_{ph}, transition energies E_{22}, and the damping parameter Γ in the two SWCNT and the DWCNT samples. The HiPco sample dispersed in SDS were studied at room temperature in Ref. 14. Relative errors are 2×10^{-3} for E_{22} and 0.1 for Γ.

	E_{ph} (meV)		E_{22} (eV)		Γ_0 (meV)		Γ_1 (meV)	
	(6,5)	(6,4)	(6,5)	(6,4)	(6,5)	(6,4)	(6,5)	(6,4)
CoMoCat	38.4	41.8	2.12	2.08	87	110	40	45
HiPco	38.4	41.8	2.11	2.07	99	74	38	52
HiPco SDS								
Refs. 14 and 26	38.4	41.8	2.18	2.11	35	35		
DWCNT	39.3	43.0	2.09	2.04	34	27	39	50

For the bucky-paper SWCNT samples, each tube is surrounded by other tubes with random chiralities. The interaction between the tubes gives rise to a distribution of transition energies, which appears as an inhomogeneous broadening of the RRS. For individual SWCNTs the environment is the same for all tubes, thus transition energies are well defined. Inner tubes in the DWCNT bucky-paper sample are embedded in an outer tube with a distinct chirality.[19,23] The inner tube transition energies are well defined for each inner-outer tube pair and Γ is not affected by inhomogeneous effects. It is thus suggested that the $\Gamma_0 \approx 30$ meV for inner tubes measures the intrinsic relaxation rate Γ_{0i} of the E_{22} optical transition.

The current data for Γ also account for the observation of the extremely large Raman cross section of inner tubes as compared to SWCNTs.[18,27] The factor 2 smaller Γ of inner tubes results in an approximate enhancement of a factor 16 in the Raman cross section as the latter is proportional to $[\Gamma^2(E_{ph}^2+\Gamma^2)]^{-1}$.

In conclusion, we studied the T dependent RRS on small diameter SWCNTs and inner tubes in DWCNTs. We observed the same redshift of optical transition energies and the same T dependence of the inverse optical excitation lifetime Γ irrespective of tube type. The environment gives rise to an inhomogeneous broadening of the RRS profiles, which is sample dependent. Γ for inner tubes in a bucky-paper sample of DWCNTs is small and is identical for micelle-suspended SWCNTs, which underlines the application potential of DWCNTs in optoelectronic devices.

The authors were supported by the FWF Grant No. 17345, by the EU Grant Nos. MERG-CT-2005-022103 and HPRN-CT-2002-00192, and by the OTKA Project Nos. TS049881, F61733, and NK60984. F.S. acknowledges the Zoltán Magyary programme.

*Electronic address: ferenc.simon@univie.ac.at. Present address: Budapest University of Technology and Economics, Institute of Physics and Solids in Magnetic Fields Research Group of the Hungarian Academy of Sciences, H-1521, Budapest P. O. Box 91, Hungary.

[1] R. Saito, G. Dresselhaus, and M. Dresselhaus, *Physical Properties of Carbon Nanotubes* (Imperial College Press, London, 1998).
[2] C. D. Spataru, S. Ismail-Beigi, L. X. Benedict, and S. G. Louie, Phys. Rev. Lett. **92**, 077402 (2004).
[3] F. Wang, G. Dukovic, L. E. Brus, and T. F. Heinz, Science **308**, 838 (2005).
[4] F. Wang, G. Dukovic, L. E. Brus, and T. F. Heinz, Phys. Rev. Lett. **92**, 177401 (2004).
[5] G. N. Ostojic *et al.*, Phys. Rev. Lett. **92**, 117402 (2004).
[6] A. Hagen *et al.*, Phys. Rev. Lett. **95**, 197401 (2005).
[7] C. D. Spataru, S. Ismail-Beigi, R. B. Capaz, and S. G. Louie, Phys. Rev. Lett. **95**, 247402 (2005).
[8] V. Perebeinos, J. Tersoff, and P. Avouris, Nano Lett. **5**, 2495 (2005).
[9] S. M. Bachilo *et al.*, Science **298**, 2361 (2002).
[10] J. Lefebvre, Y. Homma, and P. Finnie, Phys. Rev. Lett. **90**, 217401 (2003).
[11] A. Hartschuh, H. N. Pedrosa, L. Novotny, and T. D. Krauss, Science **301**, 1354 (2003).
[12] R. M. Martin and L. M. Falicov, *Resonant Raman Scattering* (Springer, Berlin, 1983), p. 79.
[13] H. Kuzmany *et al.*, Eur. Phys. J. B **22**, 307 (2001).
[14] C. Fantini *et al.*, Phys. Rev. Lett. **93**, 147406 (2004).
[15] H. Telg *et al.*, Phys. Rev. Lett. **93**, 177401 (2004).
[16] S. B. Cronin *et al.*, Phys. Rev. Lett. **96**, 127403 (2006).
[17] R. B. Capaz *et al.*, Phys. Rev. Lett. **94**, 036801 (2005).
[18] R. Pfeiffer *et al.*, Phys. Rev. Lett. **90**, 225501 (2003).
[19] R. Pfeiffer, F. Simon, H. Kuzmany, and V. N. Popov, Phys. Rev. B **72**, 161404(R) (2005).
[20] B. W. Smith, M. Monthioux, and D. E. Luzzi, Nature (London) **396**, 323 (1998).
[21] H. Kataura *et al.*, Synth. Met. **121**, 1195 (2001).
[22] F. Simon *et al.*, Phys. Rev. B **71**, 165439 (2005).
[23] R. Pfeiffer *et al.*, Eur. Phys. J. B **42**, 345 (2004).
[24] H. Kuzmany, *Solid-State Spectroscopy, An Introduction* (Springer Verlag, Berlin, 1998).
[25] N. R. Raravikar *et al.*, Phys. Rev. B **66**, 235424 (2002).
[26] Values of Γ with a factor 2 larger are given in Ref. 14 which was admited to result from an error in the resonance analysis.
[27] F. Simon *et al.*, Phys. Rev. Lett. **95**, 017401 (2005).